JOURNAL OF GEOPHYSICAL RESEARCH, VOL. 102, NO. C12, PAGES 26,411–26,423, NOVEMBER 30, 1997

The Greenland Ice Sheet Project 2 depth-age scale: Methods and results

D. A. Meese,[1] A. J. Gow,[1] R. B. Alley,[2] G. A. Zielinski,[3] P. M. Grootes,[4] M. Ram,[5] K. C. Taylor,[6] P. A. Mayewski,[3] and J. F. Bolzan[7]

Abstract. The Greenland Ice Sheet Project 2 (GISP2) depth-age scale is presented based on a multiparameter continuous count approach, to a depth of 2800 m, using a systematic combination of parameters that have never been used to this extent before. The ice at 2800 m is dated at 110,000 years B.P. with an estimated error ranging from 1 to 10% in the top 2500 m of the core and averaging 20% between 2500 and 2800 m. Parameters used to date the core include visual stratigraphy, oxygen isotopic ratios of the ice, electrical conductivity measurements, laser-light scattering from dust, volcanic signals, and major ion chemistry. GISP2 ages for major climatic events agree with independent ages based on varve chronologies, calibrated radiocarbon dates, and other techniques within the combined uncertainties. Good agreement also is obtained with Greenland Ice Core Project ice core dates and with the SPECMAP marine timescale after correlation through the $\delta^{18}O$ of O_2. Although the core is deformed below 2800 m and the continuity of the record is unclear, we attempted to date this section of the core on the basis of the laser-light scattering of dust in the ice.

Introduction

In the study of geologic materials containing paleoclimatic records, it is imperative that there be a means of dating the material. In most cases, some type of radioisotopic dating has been used, such as ^{14}C or U/Th. The dating of some materials has been obtained using chemical dating techniques combined with counting of annual layers, i.e., tree rings, corals, and lake/ocean sediment varves. While some terrestrial deposits can represent accumulations over long periods of time, very few contain identifiable annual signals that allow for accurate dating of these deposits.

Glaciers and ice sheets receive an annual net accumulation that is a combination of accumulation from precipitation and wind-blown deposition and losses due to sublimation, melt, and erosion by wind. Contained within this accumulation record are chemical signals and the manifestation of ongoing physical processes that may provide annual or seasonal indicators. On most glaciers and ice sheets, annual or seasonal signals can be altered by melt, missing years due to lack of or low accumulation rates, sublimation, wind, or a combination of these. At the Greenland Ice Sheet Project 2 (GISP2) site, where accumulation is high (approximately 0.24 m ice/yr), missing years due to deflation by wind or sublimation are unlikely. The stratigraphic record at Summit, Greenland, occasionally reveals periods of very minor melt [*Alley and Anandakrishnan*, 1995] but no more than about once per century. The GISP2 core may thus be expected to yield a long, high-quality timescale.

We have identified several parameters exhibiting annual signals and used these in combination to determine a chronology for the GISP2 ice core. The nature of these parameters, how they compare to each other, and the strengths and weaknesses of each as a dating tool are described in detail below. Additionally, means of verification of this depth-age scale and comparisons with published dates of major climatic events are discussed.

Methods

Age dating of the GISP2 ice core was accomplished by identifying and counting annual layers using a number of physical and chemical parameters that included measurements of visual stratigraphy, electrical conductivity method (ECM), laser-light scattering from dust (LLS), oxygen isotopic ratios of the ice ($\delta^{18}O$), major ion chemistry, and the analysis of glass shards and ash from volcanic eruptions. Each of these parameters (with the exception of volcanics) exhibits a distinct seasonal signal.

The definitive summer stratigraphic signal at the GISP2 site occurs in the form of coarse-grained depth-hoar layers formed by summer insolation [*Alley et al.*, 1990]. In the region around the GISP2 site the relief of the snow surface is remarkably flat. Sastrugi several centimeters in height may be produced by storms, but subsequent deposition, sublimation, and densification tend to level the surface. Depth-hoar sequences were readily recognized in snow pits dug near the GISP2 drilling site [e.g., *Shuman et al.*, 1995] (Figure 1).

Recognition of the summer and winter stratigraphic sequences in the snow pits provided important information in identifying stratigraphy in the ice core. In the core-processing

[1]U.S. Army Cold Regions Research and Engineering Laboratory, Hanover, New Hampshire.
[2]Earth System Science Center, Pennsylvania State University, University Park.
[3]Climate Change Research Center, Institute for the Study of Earth, Oceans and Space, University of New Hampshire, Durham.
[4]Leibniz Laboratory Christian Albrechts University Kiel, Kiel, Germany.
[5]Department of Physics, State University of New York at Buffalo.
[6]Desert Research Institute, University and Community College System of Nevada, Reno.
[7]Byrd Polar Research Center, Ohio State University, Columbus.

Paper number 97JC00269.
0148-0227/97/97JC-00269$09.00

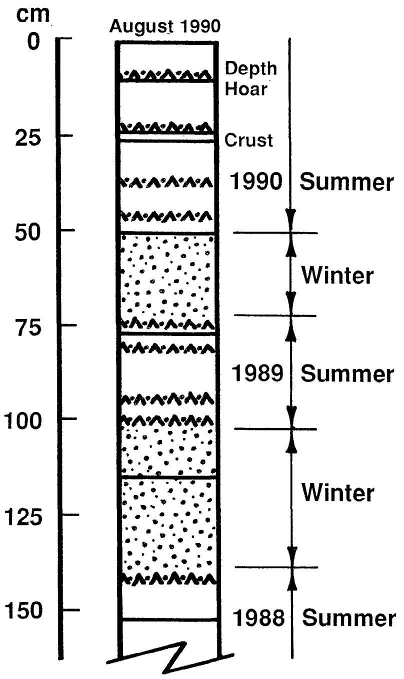

Figure 1. Stratigraphic layering of a 1.5-m snow pit excavated near the GISP2 drilling site in August 1990. The summer and winter stratigraphic sequences are readily delineated. Summer stratigraphy is dominated by layers of depth hoar which were utilized as the primary marker for delineating annual layers in dating the top 50% of the ice sheet at GISP2.

line at the GISP2 Summit site, sections of ice were cut from the core lengthwise for chemical and isotopic analysis. The cut surface on the remainder of the core was microtomed for ECM analysis. This microtoming also provided a smooth, uniform surface for stratigraphic analysis. Annual layering in the upper portions of the core is easily recognized in transmitted light. In the event of scoring on the outside of the core incurred during drilling or if the layering became faint, small "windows" were cut on the bottom side of the ice (parallel to the microtomed surface) to enhance visibility. Stratigraphy in the form of depth-hoar layer sequences remained continuous through the Holocene and into the glacial transition. During the Wisconsinan glacial the stratigraphic signal was not the characteristic depth hoar sequence of the Holocene but rather cloudy bands resulting from significant changes in seasonal dust concentration in the ice. Overlap of the two types of annual layer signal and successful calibration between the two in Preboreal ice is described by in *Alley et al.* [this issue (a)].

The ECM provides a continuous high-resolution record of low-frequency electrical conductivity of glacial ice, which is related to the acidity of the ice [*Hammer*, 1980; *Taylor et al.*, 1992]. The measurement is based on the determination of the current flowing between two moving electrodes with a potential difference of a few thousand volts. Strong inorganic acids such as sulfuric acid from volcanic activity and nitric acid controlled by atmospheric chemistry cause an increase in current. Conversely, when the acids are neutralized due to alkaline dust from continental sources or from ammonia due to biomass burning, the current is reduced [*Taylor et al.*, 1992]. As such, results from ECM can be used for a number of different types of interpretations. The most important feature of the ECM data in relation to the depth-age scale is the spring/summer acid peak from nitric acid production in the stratosphere [*Neftel et al.*, 1985]. Although ECM is an excellent seasonal indicator, as stated above, nonseasonal inputs from other sources may cause additional peaks which could be confused with the annual summer signal. In addition to being an annual indicator, ECM is also used for rapid identification of major climatic changes [*Taylor et al.*, 1993a, b] and has proved very useful in the identification of volcanic signals.

During the late spring and summer in Greenland, there is an influx of dust [*Hamilton and Langway*, 1967]. This dust peak is in part a result of dust storms that occur in both hemispheres during the spring/summer period [*Ram and Illing*, 1994] and atmospheric circulation changes which enable the stratospheric load to reach the troposphere. Dust particles in solid ice and ice meltwater scatter incident light, and the intensity of light scattered at 90° to the incident light direction is proportional to the mass of suspended particulates [*Hammer*, 1977; *Ram and Illing*, 1994; *Ram et al.*, 1995]. Liquid and solid LLS measurements were compared in several meters of core to a depth of 1812 m and matched very closely. These comparisons indicate that the solid LLS method can be used as an annual layer indicator in the Holocene and Wisconsinan even though the signal changes from one of depth hoar to layers of increased dust concentration. The solid measurements are also consistent with both ECM and visible stratigraphy in this region of the core. LLS was a very valuable dating tool throughout almost the entire length of the core, particularly in the deeper ice at GISP2, where the other techniques either fail or become increasingly unreliable. However, an increased particulate concentration may not be restricted to the spring or summer and additional influxes of dust may occur during any part of the year, creating additional peaks of a nonannual nature. The LLS signal can also be used as an indicator of major climate changes and of some volcanic events.

Additionally, $\delta^{18}O$ values (the relative difference between the $^{18}O/^{16}O$ abundance ratios of the ice and Vienna standard mean ocean water (V-SMOW) expressed in per mil (‰) of the ice) [*Epstein and Sharp*, 1959; *Dansgaard*, 1964; *Grootes et al.*, 1993] were used to identify seasonal cycles between the surface and 300-m depth in conjunction with the stratigraphic, ECM, and LLS techniques. While continuous seasonal isotope sampling remained a viable dating technique in the top 300 m of the core, the effects of diffusion rapidly obliterated the seasonal signal in deeper ice.

Many volcanic eruption signals, including both volcanic aerosols (primarily identified as H_2SO_4) and tephra, were identified throughout the core [e.g., *Zielinski et al.*, 1994, this issue], thereby providing definitive tie points to which the annual layer counting could be compared (Table 1). Of particular importance were volcanic signals found during the period of historically dated eruptions (i.e., over the last 2000 years with the A.D. 79 eruption of Vesuvius being the oldest and largest explosive eruption dated based on historical records [*Zielinski*, 1995]). There is some lag between the time of the eruption and deposition at the site which may introduce a 1- to 3-year error in the dating of the volcanic signals [*Stuiver et al.*, 1995]. As the lag is not consistent, a specific time frame cannot be generally assigned to account for this. Deposition from the 1912 Katmai eruption did arrive in 1912. However, Laki lags 1 year and the signal that is probably related to the 1600 eruption of Huaynaputina lags 3–4 years [*Zielinski*, 1995]. Although we are able to link many of the volcanic aerosol signals (SO_4^{2-} and ECM [*Zielinski et al.*, this issue]) to a specific eruption with a fairly high degree of confidence, it is locating and identifying volcanic glass from that same eruption that verifies the volcanic signal and thus the absolute age of the particular ice layer. Tephra has been found in the GISP2 core with a composition closely matching that of the candidate eruption for five of the tie points listed in Table 1. Although there was an absence of glass shards from the Vesuvius eruption in the GISP2 core, the known record of volcanism fails to provide another likely candidate. Another very large volcanic signal (third largest of the last 5000 years) that has been dated at 53 B.C. in the GISP2 core was also observed and subsequently dated as 50 B.C. in the Camp Century core [*Hammer et al.*, 1980], further validating the GISP2 chronology. In the case of the GISP2 core, layer counts closely matched the dates of all the historical eruptions given in Table 1 with the exception of Eldgja. In this instance, layer counting of the GISP2 core gives an age of A.D. 938 [*Zielinski et al.*, 1995] as opposed to A.D. 934 reported in the literature [*Hammer et al.*, 1980; *Hammer*, 1984], which is within the calculated error of 1% at this depth. It is important to note that the timing of the Eldgja eruption event at A.D. 934 is based on other ice-core records from Greenland and is not an actual historical eruption date. Similarly, the A.D. 1259 event (source volcano unknown) has been observed in ice cores from both polar regions [*Langway et al.*, 1988; *Palais et al.*, 1992]. Tephra was found in the GISP2 core for five of the eruptions listed in Table 1 [*Palais et al.*, 1991, 1992; *Fiacco et al.*, 1994; *Zielinski et al.*, 1995]; those not found include Huaynaputina, Hekla, and Vesuvius. The Huaynaputina and Hekla signals have been identified in other ice cores from Greenland [e.g., *Hammer et al.*, 1980], and the Huaynaputina eruption has also been identified in an Antarctic core [e.g., *Moore et al.*, 1991].

In certain sections of the GISP2 core, changes in the properties and mechanical condition of the core, in addition to changes in climate, have resulted in variations in the time stratigraphic parameters to the extent that some proved more valuable for annual layer dating than others. In the region of the core designated the brittle ice zone [*Gow et al.*, this issue] that occurred between 600 and 1400 m, relaxation stresses exceed the tensile strength of the ice, leading to widespread fracturing of cores [*Gow*, 1971; *Gow et al.*, this issue]. Freshly cored ice in this zone is very brittle and must be allowed to "relax" for several months before it can be processed. The fractured ice in this zone often made it difficult to apply the ECM and LLS methods. The glacial/interglacial and stadial/interstadial transitions are another example of sections where all properties exhibit large changes. A third example is the occurrence of deformed ice in the bottom 250–350 m of the core. The nature of the changes in the time-stratigraphic parameters and the effect on the dating are described in more detail below. Our ability to intercalibrate multiple annual indicators in the upper part of the core and learn their signal characteristics allowed us to retain considerable confidence in our interpretations even after some indicators were lost with increasing depth.

Table 1. List of Volcanoes Used as Tie Points to Verify the Dating of the GISP2 Core Throughout Recorded History

Volcano	Year of Eruption (A.D.)
Katmai	1912
Laki	1783
Huaynaputina	1600
Oraefajokull	1362
1259 event	1259
Hekla	1104
Eldgja	934
Vesuvius	79

Table 2. Error Estimates of the GISP2 Depth-Age Scale

Depth, m	Age, years B.P.	Parameters	Estimated Error, %
0–300	1,133	S, D, E, V, some L	1
300–719	3,289	S, E, L	1
719–1371	8,021	S, some E and L	2
1371–1510	9,374	S, E, L	2
1510–2250	39,852	S, some E and L	2
2250–2340	44,583	S, some E and L	5–10
2340–2500	56,931	L, some S and E	10
2500–2800	110,694	L, some S	20
2800–3030	161,313	L, some S	?

S, stratigraphy; D, isotopes; E, ECM; L, LLS; V, volcanics.

The greatest number of the parameters exhibiting an annual signal remained viable in the upper portion of the core (0–600 m) prior to the onset of the brittle ice zone and particularly in the top 300 m where $\delta^{18}O$ also retained an identifiable annual signal. As each of the signals carries its own structure or patterns of change, this provided an opportunity to determine the precise characteristics of each signal and the way in which they intercompared. Because this structure or pattern representing annual signals was determined for each parameter, the counting of layers could be continued down the length of the core. It is important to note that each parameter is affected by extraneous or miscellaneous events, such as volcanic eruptions, forest fires, etc., that may influence the timing and intensity of the signal. With time and experience the effects of these events on the annual signals were determined and taken into account. This was particularly important when fewer parameters were available and was the primary reason why it was so critical to use more than one parameter wherever possible in obtaining an accurate depth-age scale. The visual stratigraphy was a consistent parameter throughout most of the core. ECM and LLS were more valuable in some sections than others depending on the atmospheric chemistry and climate at that time (Table 2). Continuous examination also was essential to follow changes in annual signals as well as to characterize the climate variability fully and to avoid interpolation errors [cf. *Ram and Koenig*, this issue].

Visual stratigraphy was examined and substantially completed in the field. This stratigraphic record provided an excellent preliminary depth-age scale and an immediate indication of accumulation rate changes. A number of people contributed to this aspect of the field program [*Alley et al.*, this issue (a)]. A summer stratigraphic horizon was defined as the midpoint of the summer depth-hoar sequence and was chosen as the definitive annual layer marker. All depth-hoar sequences and other stratigraphic features (wind crusts, melt layers, etc.) were recorded on meter-long paper at a 1:1 scale. During each field season, comparisons were continually being made between ECM and stratigraphy and with LLS when available. These comparisons provided immediate information on variations in accumulation and ice-core chemistry. Additionally, they confirmed that all parameters were varying synchronously and could continue to be used in the development

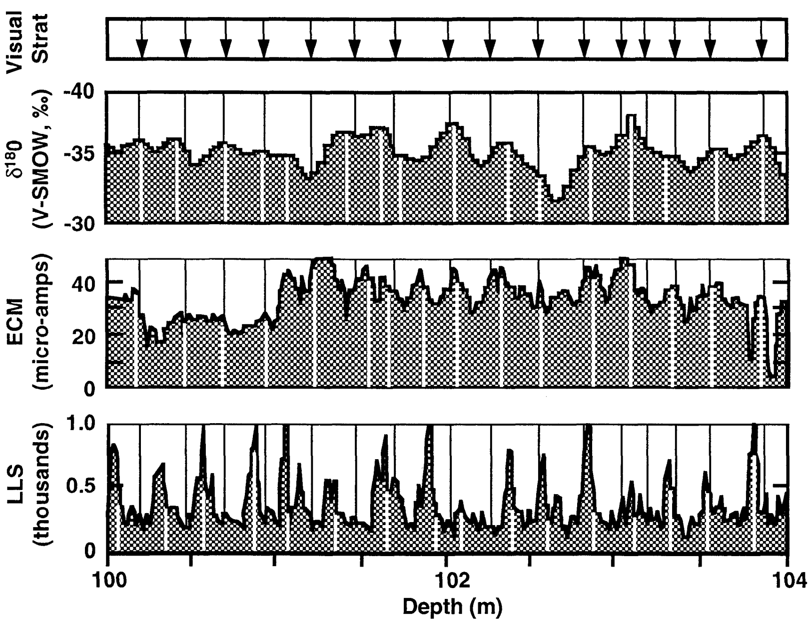

Figure 2. Example of multiparameter comparisons between 100 and 104 m. Each parameter in this sequence yielded 16 years of accumulation. Lags and leads between the parameters are evident and expected as timing of the seasonal inputs varies slightly between years and between parameters.

of the depth-age scale. After each field season the summer (annual layer) signatures for each of the other parameters were identified and recorded from peaks (or the midpoint of groups of peaks) on data plots. The summer picks for each parameter were chosen independently of other parameters in order to minimize subjective determinations. The initial picks for all parameters were placed in a spreadsheet and compared line by line or year by year. Slight lags or leads occurred due to differences in the timing of the signal of each parameter. When extraneous peaks occurred within one parameter that could not be correlated with another parameter, they were discounted. If two or more parameters showed a strong peak at essentially the same depth that could not be discounted by events such as volcanic activity or an additional influx of dust, etc., it was counted as a year even in the infrequent absence of a strong stratigraphic signal. Informed decisions were made on a year-by-year basis by the senior author, based on the weight of the available evidence. Most were either rechecked or picked independently by A.J.G., and for some sections, particularly the upper 300 m, a "round-robin" discussion involving several authors was used (particularly R.B.A. and K.C.T.). This was done to ensure that subjective determinations or biases were kept to a minimum. Additionally, much of the stratigraphy was reexamined independently by three of the authors (D.A.M., A.J.G., and R.B.A.) at the National Ice Core Laboratory (NICL) in Denver, Colorado. Since our primary stratigraphic signal based on depth-hoar formation can only occur during the summer, the midpoint of the stratigraphic layer was used as the marker depth for each summer or annual signal.

Comparison of the various signatures shows a remarkable correspondence of peaks throughout the upper 2300 m of the core. Examples of this are given in Figures 2–8, where the picks for each parameter used in the layer counting for that particular section are shown. In each figure the arrows in the top bar indicate midsummer stratigraphic picks. The lower plots include some or all of the following: $\delta^{18}O$, ECM, and/or LLS. The white lines in the shaded areas represent the summer picks for that parameter. The black lines in the upper portion of each box represent the final summer picks based on comparison and analysis of all parameters. In each example, some lag or lead between some of the individual picks and the final picks is evident; however, there is an excellent overall correspondence between the parameters. These lags and leads are attributed to variations in timing of the "summer" inputs that may encompass 2 or 3 months of the summer period [*Taylor et al.*, 1992]. For example, in the section 100–104 m (Figure 2), some lag or lead in the parameters is evident; however, the total numbers of years determined for each parameter is 16.

From 270 to 275 m (Figure 3), 20 stratigraphic (depth hoar) sequences and $\delta^{18}O$ peaks were identified in conjunction with 22 ECM and 23 LLS peaks. At one location in this sequence, $\delta^{18}O$, ECM, and LLS exhibited strong peaks that corresponded with a wind crust, but the normally diagnostic depth-hoar sequence was not identified. This was counted as 1 year in the annual layer count. The value of multiparameter counting is evident in this instance and in other sections of core where extra ECM and LLS peaks occurred that probably are not annual because these records are affected by volcanic and other events which can result in extraneous peaks. The potential for additional LLS signals is not surprising as elevated inputs of dust can occur at other times of the year, though the late spring/summer input constitutes the dominant LLS signal. The final count for the 270- to 275-m section is 21 years (± 1 year), based on the relative strength of each parameter.

An example from just above the brittle ice zone at 501–503 m is given in Figure 4. At this depth, isotopes are no longer viable as an annual indicator, so only three parameters (stratigraphy, ECM, and LLS) are used. In this instance, 11 stratigraphic markers, 12 ECM peaks, and 11 LLS peaks were identified. The final count for this 2-m section is 11. The reason for this is described fully in the caption for Figure 4. It can be seen that although the actual depths of the peaks do not align exactly, they typically record approximately the same number of years. As the depth for each parameter was recorded on a

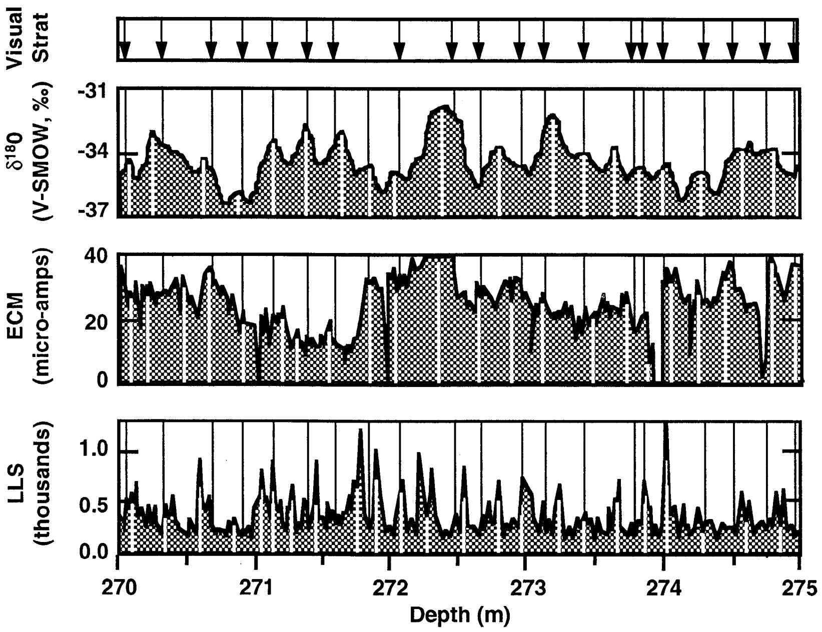

Figure 3. Multiparameter sequence between 270 and 275 m. Twenty stratigraphic layers and $\delta^{18}O$ peaks were counted in conjunction with 22 ECM and 23 LLS peaks. Annual layer markers for LLS, ECM, and $\delta^{18}O$ are shown as vertical white lines. These correspond to the spring/summer inputs for each parameter. Details of the interpretation of this record are given in the text.

computerized spreadsheet, depths were viewed continuously and peaks occurring very near meter breaks could be more easily aligned in comparison to correlations based on paper plots as in the examples given here.

The brittle ice zone (719–1371 m) was a region of some concern due to the large number of fractures in the core [*Gow et al.*, this issue]. While this fracturing of the ice core interfered particularly with the ECM and LLS measurements, visual stratigraphy remained very clear and readily decipherable in this section and constituted the primary annual layer indicator. However, scattered ECM and/or LLS data from the brittle ice zone were available, and they provided useful checks on stratigraphic layer counts. A comparison of the stratigraphic and LLS records is shown in Figure 5 between 871 and 873 m. Both parameters exhibit 12 peaks in this section, but because of lags or leads the final picks do not always coincide. It is evident that although the mechanical condition of the ice deteriorated somewhat in this region, the parameters used for layer identi-

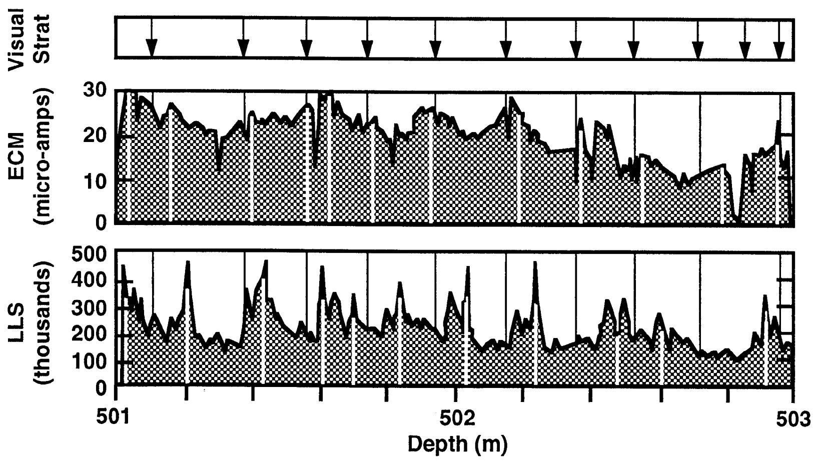

Figure 4. In this 2-m section from 501 to 503 m, 11 stratigraphic summers were identified in conjunction with 12 ECM peaks and 11 LLS peaks. A final count of 11 annual layers was determined for this 2-m section of ice. The stratigraphic sequence corresponding to the ECM and LLS peaks at 501 m is actually in the 500-m section and was counted there. At approximately 502.72 m a stratigraphic sequence is present as well as a strong ECM signal; however, the LLS signal is very weak and was not counted, resulting in an undercount in the LLS record. However, this did not affect the final count. Also, at approximately 502.9 m a stratigraphic sequence was observed, but there is not a corresponding strong ECM or LLS peak and this sequence was thus dropped from the count. Again, this section of ice shows that although the actual depths of the peaks are slightly offset, approximately the same number of years is revealed for each parameter.

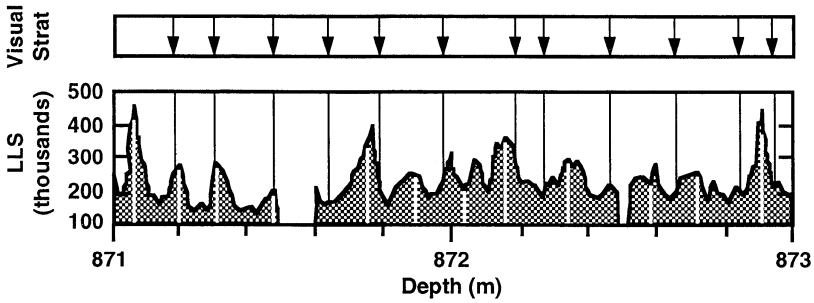

Figure 5. This section from 871 to 873 m is from the brittle ice zone. In this zone, stratigraphy was the primary annual signal indicator and ECM and LLS were used when available. In this section, 12 annual layer markers are observed in both the stratigraphy and the LLS, indicating that counting is still viable within the brittle ice zone.

fication remained sufficiently consistent to sustain annual layer counting, essentially without a break, through the brittle ice zone.

Between 1370 and 1678 m, in the Preboreal preceeding the onset of the Younger Dryas, the character of the visual stratigraphic signal changed drastically from that of the characteristic depth-hoar sequences to one consisting of alternating clear and cloudy bands with the cloudy bands containing much higher concentrations of dust than were present in younger Holocene ice. The region between 1680 and 1800 m consists of the Younger Dryas, the Bølling/Allerød, and the transition to full glacial conditions. Once into the full glacial (Wisconsinan) period, below 1800 m, dust concentrations increased significantly and the magnitude of changes seen in the ECM record decreased. As a result of this and perhaps because of limitations imposed by the spatial resolution of the ECM technique, it became increasingly difficult to use the ECM record for annual layer signal identification in deeper ice-age ice. A photograph of a 19-cm-long section of core in Figure 6 demonstrates the very distinct annual layering associated with 12 summer peaks, based on the bright white light bands corresponding to spring/summer dust rich layers in the core. A 0.5-m section of stratigraphic and LLS records from between 2247.5 and 2248.0 m is shown in Figure 7. In this core, 42 stratigraphic and 39 LLS annual peaks were identified. The difference in counts using these two techniques in this section of the record is clearly higher than in the Holocene but is still less than 10%.

Beginning around 2400 m, visual stratigraphy in extended sections of the core became so faint that the annual layer structure became very difficult to decipher. This was especially true of those sections of ice associated with Dansgaard-Oeschger events which contained greatly reduced dust levels. Because of the low dust levels, resulting in weak to nondecipherable stratigraphy, significant undercounting of annual layers occurred in the region of the GISP2 core between 2500 and 2800 m. This forced greater reliance on the LLS record in which annual layer peaks could still be readily observed. However, many sections of core between 2500- and 2800-m depth retained identifiable stratigraphy, especially those sections of ice containing elevated dust levels associated with colder climatic conditions. Such sections exhibited readily decipherable layer structure that corresponded closely with annual layer peaks derived from the LLS record.

As records were obtained, the actual depth recorded for

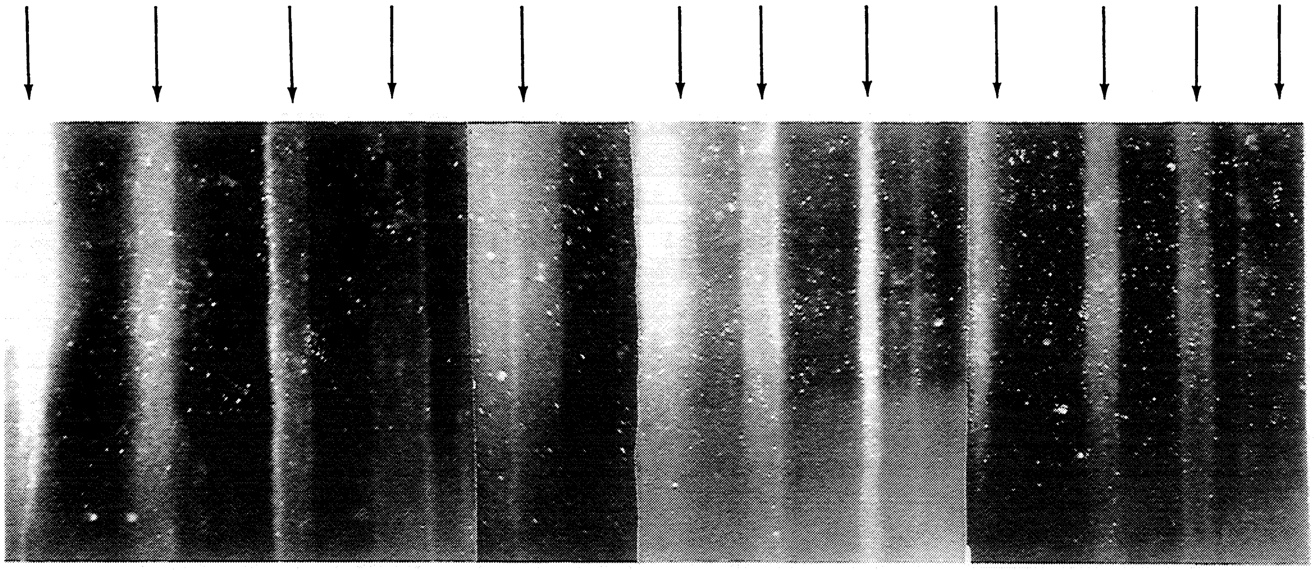

Figure 6. Photograph of a 19-cm-long section of ice from 1855 m showing annual stratigraphic layers in the Wisconsinan. This section contains 12 summer layers (arrowed) sandwiched between darker winter layers. The lighter layers are a result of increased scattering of light due to higher concentrations of dust.

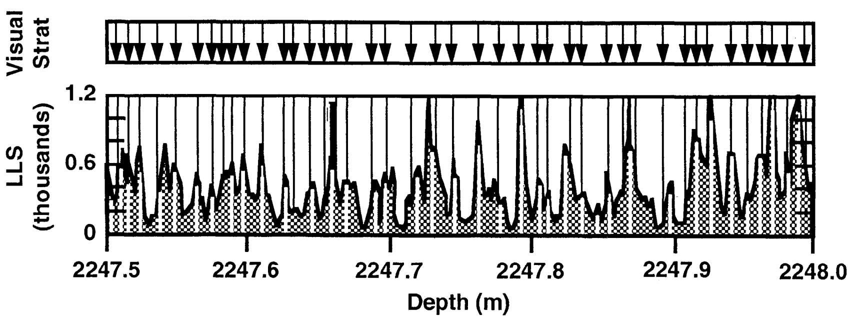

Figure 7. This section between 2247.5 and 2248.0 m shows the comparison between stratigraphy and LLS much deeper in the core. It can be seen that the methodology used from the top of the core still holds and the comparisons are excellent. In this case, there were 42 stratigraphic and 39 LLS annual layer markers identified.

each summer (or annual layer) was based on the position of the visual stratigraphic marker. The stratigraphic record was chosen because the timing of the annual signal is more clearly defined than other parameters and is typically the most consistent. In the event of weak or absent diagnostic stratigraphy, other parameters were used in the following order: isotopes (0–300 m), ECM, and LLS. In instances where core loss occurred [*Gow et al.*, this issue; *Greenland Ice Sheet Project 2 Science Management Office*, 1993], approximate annual depths were interpolated by using the average value of the number of annual layers in an equivalent amount of core above and below the area of loss. Although this results in loss of detail of the annual variation in the accumulation record throughout these areas, we believe that the overall chronology is not seriously affected.

It is believed that viable dating is retained to 2800 m below which flow disturbance in the ice becomes quite severe [*Alley et al.*, 1995; *Gow et al.*, this issue]. Sowers and Bender developed a correlated timescale [*Bender et al.*, 1994] in which an inverse correlation technique was used to map the record of $\delta^{18}O$ in atmospheric O_2 ($\delta^{18}O_{atm}$) from GISP2 into the Vostok $\delta^{18}O_{atm}$ that has been tied to the SPECMAP ocean timescale [*Sowers et al.*, 1993]. They predicted the age of the ice at 2800 m to be about 110,000 years, 25,000 years older than had been originally counted on the basis of visual stratigraphy [*Meese et al.*, 1994]. The preliminary depth-age scale derived from the analysis of the visual stratigraphy below 2200 m [*Meese et al.*, 1994] and the Sowers-Bender correlated timescale started to deviate at 2341 m.

Because of the above discrepancy the senior author returned to the National Ice Core Laboratory and rechecked the visible stratigraphy. No significant changes from the original counts were observed. Study of the LLS record, now available in a more detailed format using a 1-mm beam width rather than 8

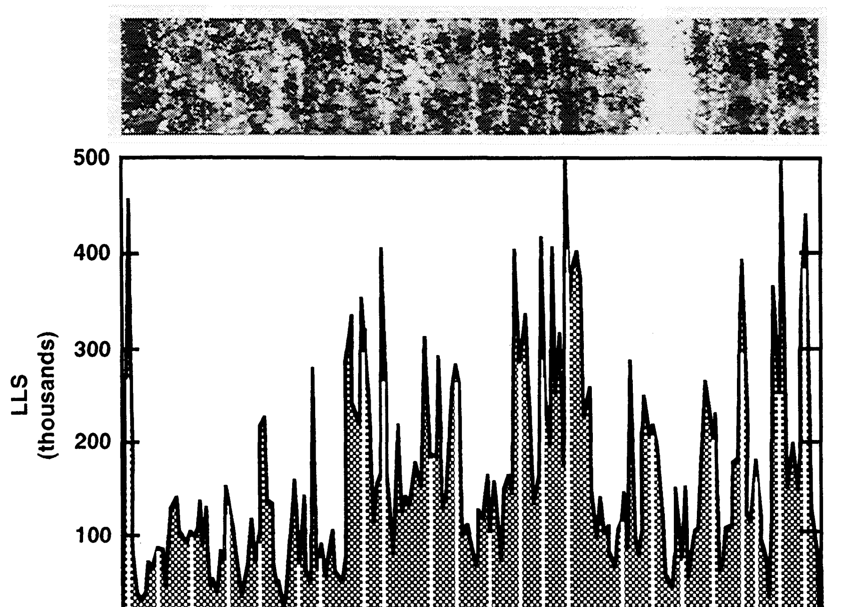

Figure 8. A thin section photograph taken between crossed polarizers showing stratigraphy in a section between 2552.60 and 2552.80 compared to the LLS record. Most of the bright white layers (containing elevated levels of dust) compare closely to the peaks in the LLS record.

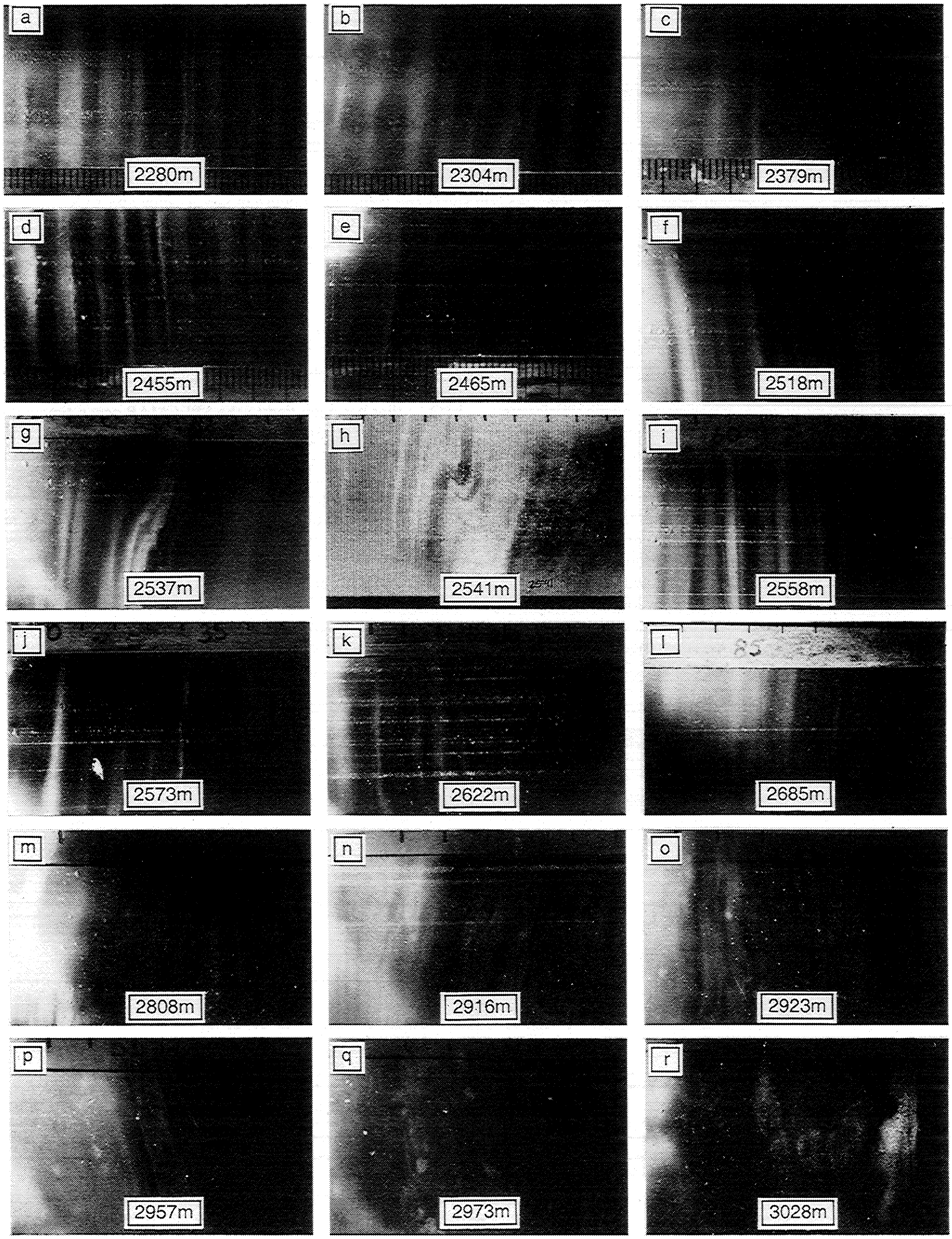
a
2280m
b
2304m
c
2379m
d
2455m
e
2465m
f
2518m
g
2537m
h
2541m
i
2558m
j
2573m
k
2622m
l
2685m
m
2808m
n
2916m
o
2923m
p
2957m
q
2973m
r
3028m

mm [*Ram and Koening*, this issue], showed there was more structure indicating a greater number of annual layers, leading to a more expanded timescale than had been interpreted from the stratigraphic record. Therefore the entire high-resolution LLS record between 2300 and 2800 m was reexamined independently by two of the authors (D.A.M. and A.J.G.). Dating of the GISP2 core by LLS is ultimately limited by the spatial resolution of the measurement technique (currently 1 mm). Several points are required to identify a definitive peak; for the LLS method the minimum thickness necessary for successful identification of an annual layer is 3 or 4 mm (requiring four or five points to identify the peak). Layers less than 3 mm thick could be missed, however, leading to undercounting. The potential for undercounting annual layers in the stratigraphic record is known to exist in low accumulation areas such as the south pole [*Gow*, 1965]. However, such undercounting due to extreme low accumulation years or hiatus years is estimated by Gow not to exceed 10%. The solid ice LLS instrument used on the GISP2 core [*Ram and Koenig*, this issue] was configured to produce 1000 readings per meter for most of the deeper core; hence the theoretical maximum number of annual layers that could be identified in a meter of core is somewhat below 500.

A photograph of a thin vertical section of ice between 2552.6 and 2552.8 m and its relationship to the LLS record is shown in Figure 8. In this section of ice, photographed between crossed polarizers to reveal differences in the dust-related sizes of crystals in the summer and winter layers, 21 stratigraphic sequences were identified and 23 LLS peaks were counted. As opposed to the regions of the core above 2500 m, where the number of layers counted varied between parameters without a definitive trend, below 2500 m the number of LLS layers was consistently higher than the number identified by visible stratigraphy, based on the peaking characteristics of the LLS record. A comparison of counts in years per meter shows that the overall structure of the LLS record is very similar as determined by both individuals, but with one person consistently counting on average 20% higher than the other. To obtain a final GISP2 depth-age scale, the two sets of counts were then averaged. This average was then compared to the Sowers-Bender correlated timescale and showed a maximum difference of 1.1% with an age of approximately 111,000 years B.P.

Comparisons were also made between the counts, the ECM record, and the $\delta^{18}O$ record. A good correspondence exists between the layer counts, the ECM, and the $\delta^{18}O$ record, indicating that the LLS record in this region of the core continues to track the climatic signal and that the annual layer record still remains intact. It is clear that the original examination of the visual stratigraphy led to undercounting below 2400 m. Reexamination of a number of core sections indicates that undercounting very likely results from either the thinning and merging of layers or the fact that the eye could no longer distinguish individual layers, especially in cores exhibiting very faint stratigraphy related to low dust levels. Complications arising from layer deformation are another possibility. Very small folds and waves in the layers were observed as high as 2487 m, but these are not likely to have caused disruption of the orderly stratigraphic record. However, in the event of more severe deformation, stratigraphic succession could have been disrupted to the point where it becomes impossible to distinguish and/or count individual layers.

As stated earlier, various combinations of parameters based on the chemical and physical properties of the ice were used throughout the length of the core to evaluate the depth-age scale. Table 2 lists the depth and age ranges for different combinations of layer-counting parameters and error estimates.

It has been reported elsewhere [*Alley et al.*, this issue (a) *Ram and Koenig*, this issue] that counting limited to only on(parameter or to the counting of 1 m in every 5 (or 20% provides nearly as accurate a timescale as the multiparametei continuous count method. Stratigraphic layer counting yields timescale that is within 1% of the multiparameter method i the Holocene and even deeper. However, deeper in the coi the difference between the one parameter and multiparamet(methods tends to increase and much of the fine detail that cε only be obtained by continuous counting methods is likely be missed. Variations in annual layer thickness can be read seen on an annual basis when continuous counting is coı pleted. For example, when layer counting is limited to only o method, i.e., stratigraphy in the upper 2300 m of the core more subjective approach is taken in rejecting the extreı years from the record. Not only do these extreme years ex they may indicate short-term changes, particularly if th trends persist for more than a number of years. A compari: of all parameters sometimes reveals peaks of a nonann nature, for example, peaks related to volcanic events, whic included in the count would result in overcounting. In addit to identifying short-term trends, the multiparameter apprc identifies variations which may be occurring in only one rameter. As indicated earlier, a prime example is the prot of undercounting of layers associated with large section core exhibiting merged layers or very faint visual stratigrε below 2500 m. The resultant large difference in the times

Figure 9. (opposite) Examples of annual layer structure seen in GISP2 ice cores illuminated from below by a fiber optic light source. Examples of both undisturbed and disturbed stratigraphy are shown. (a) 2280 m. Distinctive annual layer structure. (b) 2304 m. Less distinctive annual layering due to decreasing dust levels in the ice. (c) 2379 m. Even less distinctive layering due to the decreased dust content of the ice; layers are more widely spaced indicating higher annual snowfall. (d) 2455 m. Return to more distinctive annual layering. (e) 2465 m. The fewer layers in this core indicate a higher accumulation rate associated with lower dust content, indicating a warmer climate than at 2455 m. (f) 2518 m. There are more layers in this section, indicating lower accumulation and a cooler climate. Layers are still fairly horizontal with some minor waviness. (g) 2537 m. A minor disturbance is evident with a small z-fold near the bottom of the photograph. This fold is small enough that it did not disturb the climatic record or the layer counts. (h) 2541 m. Prominent folding of annual layers in the ice. However, layer counts are still decipherable. (i) 2558. Return to undisturbed annual layering. (j) 2573. Distinctive annual layer structure; some minor waviness of layers evident. (k) 2622 m. Some minor waviness or bending of the layers in evidence in this core. (l) 2685 m. Annual layers becoming very closely spaced in this core. (m) 2808 m. Layer structure still discernible but difficult to count. (n) 2916 m. Layer structure very disturbed and discontinuous; annual layering is no longer discernible. (o) 2923 m. Layer structure disturbed and discontinuous; no discernible annual layering. (p) 2957 m. No definitive annual layering present; sections of cloudy ice alternate with clear ice, and layers are curved and discontinuous. (q) 2973 m. Highly compressed layer structure; layers do not appear to be deformed. (r) 3028 m. Intermixing of cloudy and clear ice; no discernible layering present.

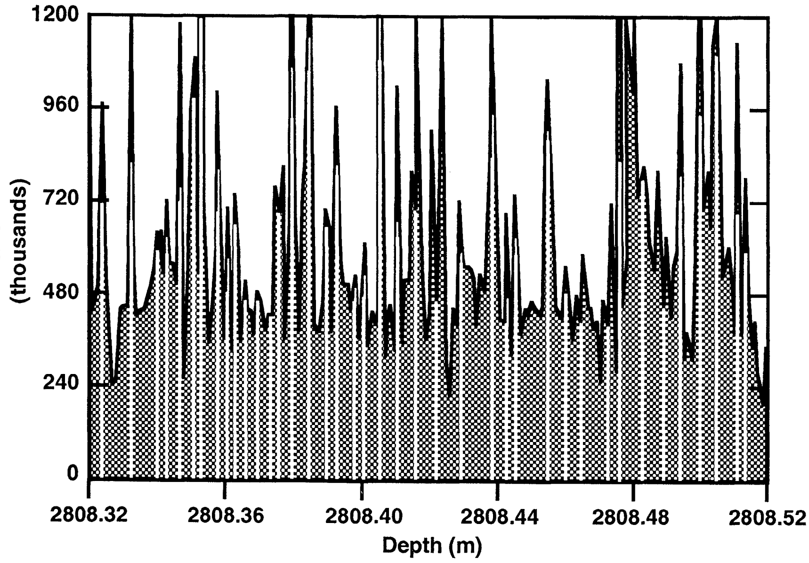

Figure 10. Example of an LLS record from 2808 m. Some faint stratigraphic layering is decipherable in this meter of core and appears to be disturbed. Even though the stratigraphic record is disturbed in this section of core, the LLS record appears to be intact, and its overall character is identical to that observed in undisturbed ice at higher levels in the ice sheet.

based on the original visible layer counts, compared with the Sowers-Bender correlated scale provided the impetus to reexamine the visual stratigraphy in greater detail in conjunction with the LLS record. This reanalysis has resulted in what we believe is a much more accurate scale than we previously had obtained.

The region below 2800 m has been a subject of much discussion based on the conclusion from the Greenland Ice Core Project (GRIP) core that the interglacial climate during the Eemian had been unstable. This was put into doubt when it was realized that the profiles of isotopes and other core properties from the GISP2 and GRIP cores no longer agreed. At depths below 2800 m, two major complications, loss of a consistent visible stratigraphic signal and possible lack of sufficient spatial resolution to resolve the annual layering, limit our ability to identify annual layers. The stratigraphic record revealed evidence of appreciable deformation in this region of the core. Examples of overturned folds, z folds, highly inclined layers, and other structural features indicating disruption of stratigraphic order are abundant (Figure 9). These deformational features include reversals in the direction of inclined layering in sections of core up to 1 m long, which could indicate overturned folds. Some interpretation of the structures in this region has been presented [*Alley et al.*, this issue (b); *Gow et al.*, this issue], but much more work is needed to determine the precise nature and extent of the deformation. It is likely that this area of the core also contains structural discontinuities. Such discontinuities could arise from the deposition of one ice sheet on top of remnants of previous ice sheets, leading to significant time gaps in the stratigraphic record. In theory it is possible to identify ice from a single age that has been folded sufficiently to be duplicated in the core by searching for ice at two depths that have the same chemical, isotopic, and gas characteristics. In practice, however, depositional spatial variability, diffusion, and measurement limitations are likely to make identification of repeated sections difficult to resolve. We have not identified any large repeated sections, but we consider it possible that duplicated sections exist.

The diagnostic features of the LLS record (on which we relied heavily to evaluate annual layer counting between 2500 and 2800 m) appear to be retained in the ice below 2800 m, and for this reason alone, layer counting was continued to a depth of 3030 m. Given the widespread evidence of disturbed structure in the ice, it is clear that the layer count is very unlikely to be continuous. Yet, it provides information on the sections of apparently little disturbed ice in the deformed region of the core, including the number of years contained in each of those sections.

An example of the clarity of the LLS record obtained at 2808 m is shown in Figure 10. Faint banding indicative of annual layering was still discernible at this depth. Examples of the LLS record shown in Figures 11 and 12 are of sections of ice exhibiting significantly different stratigraphic structure. At 2840 m (Figure 11) the ice was very clear and coarse grained with very little stratigraphic structure visible. At 2850 m (Figure 12), where identifiable layering briefly reappeared, the ice was much finer grained. The reappearance of visual stratigraphy in conjunction with the formation of fine-grained ice is entirely compatible with the increased dust concentrations evident in the vertical scale of the LLS record. To determine the number of layers between 2800 and 3030 m, the senior author (D.A.M.) counted continuously to 3030 m, approximately 10 m above the silty ice contact. Another one of the authors (A.J.G.) counted continuously to 2850 m and then 1 m in every 5 m to 3030 m. Interpolations were then made in this latter record in order to compare the counts of both observers on a relative basis. More structure is evident in the counts made by D.A.M., showing the importance of counting continuously. Nonetheless, the average variation in the two sets of counts was 20% on a layer per meter basis between 2500 and 2800 m and 24% between 2800 and 3000 m. At 2800 m the age of the ice is determined to be 110,693 years B.P. ±10%. The number of layers obtained by averaging the counts of the two observers between 2800 and 3030 m is 50,600 with an unknown error. Because of deformation and likelihood of discontinuities, it is not possible to assign a timescale or ages to this region of the

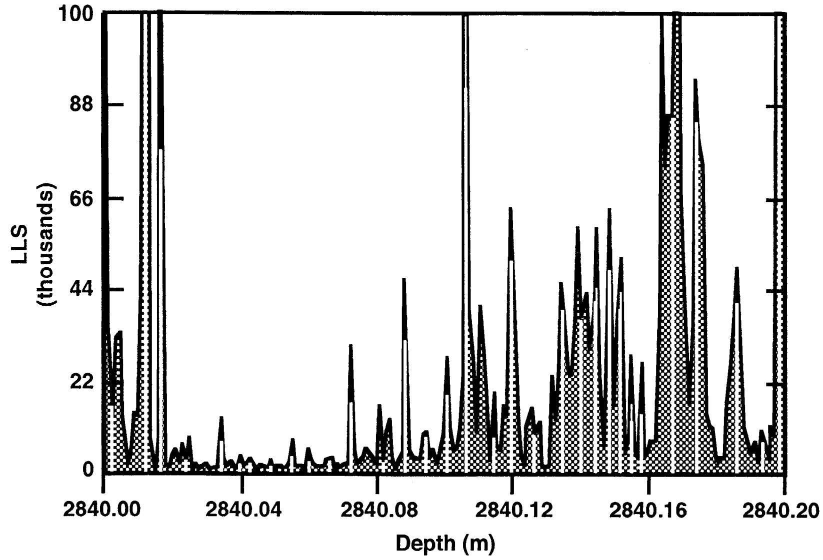

Figure 11. An example of the LLS record from ice that is very clear and coarse grained with little visible stratigraphy.

core. If future work allows us to deconvolve this area of the core, we may be able to identify climatic events and place age limits on them.

Error and Verification

Putting error estimates on the depth-age scale is difficult. The accuracy of the depth-age scale can be checked against historically dated volcanic events over the last 2000 years (i.e., tie points; Table 1). If a discrepancy existed between the date of a known volcanic eruption and the corresponding date assigned on the basis of elevated ECM and sulfate peaks, the strengths of the various annual signals were then reevaluated to determine if perhaps a more accurate date could be obtained. Most of our final dates of the major historical volcanic eruptions identified in the core match stratigraphically defined dates precisely. To obtain an estimate of error based on the original layer counting, the volcanic signals were examined in relation to the age scale before any reevaluation of the years was completed. The worst case was for Vesuvius (A.D. 79). Analysis of the GISP2 core gave a date which was 12 years older than the historical eruption date. This difference results in a 0.63% error, which is less than the 1% stated for this work.

Assessing the accuracy of our depth-age scale based on the multiparameter approach in deeper ice becomes increasingly more difficult as there are no independent means of dating the ice by radiometric techniques. Possible comparisons might be made with events that have been dated in corals and deep-sea cores, but these events likely have larger errors than those applying to the GISP2 timescale. Additionally, a depth-age scale exists for the European GRIP core (largely based on flow modeling and noncontinuous methods) which can also be used for comparison. The errors that are listed in Table 2 are based

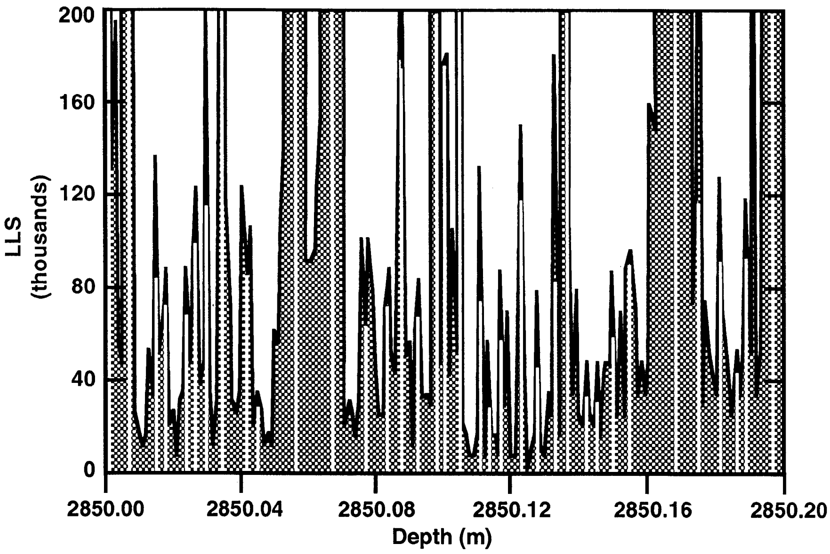

Figure 12. An example of the LLS record from ice that contains decipherable stratigraphic layering and is much finer grained than the section of ice presented in Figure 11.

on variations noted between methods and between analysts. All of these estimates are conservative and should be considered to err on the side of maximum error.

The Younger Dryas (YD)–Bølling/Allerød–Oldest Dryas sequence provides one tie point, particularly the YD termination at 1678 m where a dramatic change occurs in layer thickness (resulting in an estimated twofold to threefold change in accumulation rate), corresponding to an age of 11,640 years B.P. This agrees very closely with most published dates of around 11,500 years B.P. (a variation of slightly more than 1%) for the YD termination [*Alley et al.*, this issue (a)].

Another tie point that can be used is Heinrich Event 3 (H3) between Interstadial 4 and 5 [*Meese et al.*, 1993]. On the basis of comparisons of high-resolution deep-sea sediment records from the North Atlantic a ^{14}C date of 26,500 was obtained for core 2381 and a date of 27,000 was obtained for Orphan Knoll (G. Bond, personal communication, 1996). These dates are approximately equivalent to a calendar date of 30,000–31,000 years B.P. [*Bond and Lotti*, 1995] based on the U/Th calibration of *Bard et al.* [1990]. The date obtained from continuous counting of annual layers in the GISP2 core for H3 is 31,200 years B.P. This again provides good agreement.

A comparison can also be made between the correlated timescale presented by *Bender et al.* [1994] and the depth-age scale. The model is based on $\delta^{18}O_{atm}$ of O_2 measurements of the GISP2 ice core and compared to the Vostok ice core and SPECMAP for the oceans. At 2500 m, annual layer counts give an age equivalent to 56,930 years B.P., and the correlated scale of *Bender et al.* [1994] gives 57,600 years B.P. This difference is slightly higher than 1%. This is somewhat remarkable, since the error for both methods is estimated to be much higher than this. The same trend holds at depth, where layer counting at 2700 m gives 89,084 years B.P. compared to a model age of 89,244 years B.P. (now less than 1% variation in the two scales). Over the depth range, 2700–2800 m, an excellent correlation also exists between the $\delta^{18}O_{atm}$ in the Vostok and GISP2 cores [*Bender et al.*, 1994]. *Bender et al.* [1994] suggest that the ice below 2850 m may largely be from the substages 5e and 5d, approximately 128,000–140,000 years B.P. If the layer counts based on the LLS technique are used as dates in this section of the core, the estimated age would be 121,200 years B.P. at 2850 m, less than a 5% variation at 2850 m as suggested above, indicating that this ice may in fact be part of substages 5e and 5d. However, as stated above, caution must be exercised as the full extent of the deformation in this region has not yet been completely defined.

A final comparison is made between the GISP2 depth-age scale based on annual layer counts and the GRIP depth-age scale [*Dansgaard et al.*, 1993; *Johnsen et al.*, 1995]. The GRIP timescale back to 14,500 years B.P. was derived from annual layer counts from the surface. Dating below 14,500 years B.P. was calculated on the basis of flow modeling and chemical techniques including Ca^{2+}, NH_4^+, and microparticles [*Johnsen et al.*, 1992]. There are potential problems with both the GISP2 and GRIP timescales. Most ice flow models predict extremely rapid thinning near the bottom of an ice sheet. Annual layer counting based on LLS results at GISP2 shows that thinning does not appear to occur at the rate predicted by the models [*Schøtt et al.*, 1992; *Dahl-Jensen et al.*, 1993]. However, both the GISP2 and GRIP cores are known to exhibit evidence of severe structural disturbance in the basal 200–300 m, and this has likely led to discontinuities or breaks in the stratigraphic sequence.

Summary

The GISP2 ice core has been dated continuously from 0 to 2800 m with considerable precision. The age obtained at 2800 m was 111,000 years B.P. with an estimated error ranging from 1 to 10% and up to 20% between 2500 and 2800 m. Layer counting was extended to 3030 m on the basis of the LLS record mainly to obtain a possible age limit of the ice near its contact with the bed, assuming minimal disturbance by deformation of the stratigraphic record. Layer counts in excess of 300/m were measured in the deepest ice, and an estimated age of 161,000 years B.P. was obtained at 3030 m with an unknown error. This age estimate is significantly less than that obtained at GRIP, largely on the basis of ice flow modeling. However, it is likely that structural disturbance observed in the basal 250 m of ice at both locations has affected both the timescales to an unknown degree.

Comparison of the GISP2 depth-age scale with published dates for the termination of the Younger Dryas shows correspondence within the combined errors. Another tie point exists deeper in the core for Heinrich Event 3 at approximately 30,000 years B.P., again with excellent correspondence to published records. Below this event, correlations made with a model based on $\delta^{18}O$ of O_2 reveal a close correspondence.

Acknowledgments. The authors would like to thank the National Science Foundation Office of Polar Programs for funding of this project and the GISP2 Science Management Office, the Polar Ice Coring Office, the 109th Air National Guard, the National Ice Core Laboratory, and numerous colleagues for their assistance during the drilling and assistance in obtaining the data necessary for the depth-age scale. D.A.M. and A.J.G. also thank the USA Cold Regions Research and Engineering Laboratory for support and Army basic research projects for partial funding.

References

Alley, R. B., and S. Anandakrishnan, Variations in melt-layer frequency in the GISP2 ice core: Implications for Holocene summer temperatures in central Greenland, *Ann. Glaciol.*, *21*, 64–70, 1995.

Alley, R. B., E. S. Saltzman, K. M. Cuffey, and J. J. Fitzpatrick, Summertime formation of depth hoar in central Greenland, *Geophys. Res. Lett.*, *17*, 2393–2396, 1990.

Alley, R. B., A. J. Gow, S. J. Johnsen, J. Kipfstuhl, D. A. Meese, and T. H. Thorsteinsson, Comparison of deep ice cores, *Nature*, *373*, 393–394, 1995.

Alley, R. B., et al., Visual-stratigraphic dating of the Greenland Ice Sheet Project 2 ice core: Basis, reproducibility, and application, *J. Geophys. Res.*, this issue (a).

Alley, R. B., A. J. Gow, D. A. Meese, J. J. Fitzpatrick, E. D. Waddington, and J. F. Bolzan, Grain-scale processes, folding, and stratigraphic disturbance in the Greenland Ice Sheet Project 2 ice core, *J. Geophys. Res.*, this issue (b).

Bard, E., B. Hamelin, R. G. Fairbanks, and A. Zindler, Calibration of the ^{14}C timescale over the past 30,000 years using mass spectrometric U-Th ages from Barbados corals, *Nature*, *345*, 405–410, 1990.

Bender, M., T. Sowers, M. Dickson, J. Orchardo, P. Grootes, P. Mayewski, and D. Meese, Climate correlations between Greenland and Antarctica during the past 100,000 years, *Nature*, *372*, 663–666, 1994.

Bond, G., and R. Lotti, Iceberg discharges into the North Atlantic on millennial time scales during the last glaciation, *Science*, *267*, 1005–1010, 1995.

Dahl-Jensen, D., S. J. Johnsen, C. U. Hammer, H. B. Clausen, and J. Jouzel, Past accumulation rates derived from observed annual layers in the GRIP ice core from Summit, central Greenland, in *Ice in the Climate System*, *NATO ASI Ser. I*, vol. 12, edited by W. R. Peltier, pp. 517–532, Springer-Verlag, New York, 1993.

Dansgaard, W., Stable isotopes in precipitation, *Tellus*, *16*(4), 436–468, 1964.

Dansgaard, W., et al., Evidence for general instability of past climate from a 250-kyr ice-core record, *Nature*, *364*, 218–220, 1993.
Epstein, S., and R. P. Sharp, Oxygen isotope studies, *Eos Trans. AGU*, *40*(1), 81–84, 1959.
Fiacco, R. J., Jr., T. Thordarson, M. S. Germani, S. Self, J. M. Palais, S. Whitlow, and P. Grootes, Atmospheric aerosol loading and transport due to the 1783–84 Laki eruption in Iceland, interpreted from ash particles and acidity in the GISP2 ice core, *Quat. Res.*, *42*, 231–240, 1994.
Gow, A. J., On the accumulation and seasonal stratification of snow at the south pole, *J. Glaciol.*, *5*, 467–477, 1965.
Gow, A. J., Relaxation of ice in deep drill cores from Antarctica, *J. Geophys. Res.*, *76*, 2533–2541, 1971.
Gow, A. J., D. A. Meese, R. B. Alley, J. J. Fitzpatrick, S. Anandakrishnan, G. A. Woods, and B. C. Elder, Physical and structural properties of the Greenland Ice Sheet Project 2 ice core: A review, *J. Geophys. Res.*, this issue.
Greenland Ice Sheet Project 2 Science Management Office, GISP2 core data book, 114 pp., Univ. of N. H., Durham, 1993.
Grootes, P. M., M. Stuiver, J. W. C. White, S. Johnsen, and J. Jouzel, Comparison of oxygen isotope records from the GISP2 and GRIP Greenland ice cores, *Nature*, *366*, 552–554, 1993.
Hamilton, W. L., and C. C. Langway Jr., A correlation of microparticle concentrations with oxygen isotope ratios in 700 year old Greenland ice, *Earth Planet. Sci. Lett.*, *3*, 363–366, 1967.
Hammer, C. U., Past volcanism revealed by Greenland Ice Sheet impurities, *Nature*, *270*, 482–486, 1977.
Hammer, C. U., Acidity of polar ice cores in relation to absolute dating, past volcanism, and radio-echos, *J. Glaciol.*, *25*, 359–372, 1980.
Hammer, C. U., Traces of Icelandic eruptions in the Greenland Ice Sheet, *Joekull*, *34*, 51–54, 1984.
Hammer, C. U., H. B. Clausen, and W. Dansgaard, Greenland ice sheet evidence of post-glacial volcanism and its climatic impact, *Nature*, *288*, 230–235, 1980.
Johnsen, S. J., H. B. Clausen, W. Dansgaard, K. Fuhrer, N. Gundestrup, C. U. Hammer, P. Iverson, J. Jouzel, B. Stauffer, and J. P. Steffensen, Irregular glacial interstadials recorded in a new Greenland ice core, *Nature*, *359*, 311–313, 1992.
Johnsen, S. J., H. B. Clausen, W. Dansgaard, N. Gundestrup, C. Hammer, and H. Tauber, The Eem stable isotope record along the GRIP ice core and its interpretation, *Quat. Res.*, *43*, 117–124, 1995.
Langway, C. C., Jr., H. B. Clausen, and C. U. Hammer, An interhemispheric volcanic time-marker in ice cores from Greenland and Antarctica, *Ann. Glaciol.*, *10*, 102–108, 1988.
Meese, D. A., A. J. Gow, R. B. Alley, P. M. Grootes, P. A. Mayewski, M. Ram, K. C. Taylor, E. D. Waddington, G. A. Zielinski, and G. C. Bond, Counting down . . . the GISP2 depth/age scale, *Eos Trans. AGU*, *74*(43), Fall Meet. Suppl., 83, 1993.
Meese, D. A., R. B. Alley, A. J. Gow, P. Grootes, P. A. Mayewski, M. Ram, K. C. Taylor, E. D. Waddington, and G. Zielinski, Preliminary depth-age scale of the GISP2 ice core, *CRREL Spec. Rep. 94-1*, 66 pp., Cold Reg. Res. and Eng. Lab., Hanover, N. H., 1994.
Moore, J. C., H. Narita, and N. Maeno, A continuous 770-year record of volcanic activity from East Antarctica, *J. Geophys. Res.*, *96*, 17,353–17,359, 1991.
Neftel, A., M. Andree, J. Schwander, B. Stauffer, and C. U. Hammer, Measurements of a kind of DC-conductivity on cores from Dye 3, in *Greenland Ice Core: Geophysics, Geochemistry, and the Environment*, *Geophys. Monogr. Ser.*, vol. 33, edited by C. C. Langway Jr., H. Oeschger, and W. Dansgaard, pp. 32–38, AGU, Washington, D. C., 1985.
Palais, J. M., K. Taylor, P. A. Mayewski, and P. Grootes, Volcanic ash from the 1362 A.D. Oraefojokull eruption (Iceland) in the Greenland Ice Sheet, *Geophys. Res. Lett.*, *18*, 1241–1244, 1991.
Palais, J. M., M. S. Germani, and G. A. Zielinski, Inter-hemispheric transport of volcanic ash from a 1259 A.D. volcanic eruption to the Greenland and Antarctic Ice Sheets, *Geophys. Res. Lett.*, *19*, 801–804, 1992.
Ram, M., and M. Illing, Polar ice stratigraphy from laser-light scattering: Scattering from meltwater, *J. Glaciol.*, *40*, 504–508, 1994.
Ram, M., and G. Koenig, Continuous dust concentration profile of pre-Holocene ice from the Greenland Ice Sheet Project 2: Dust stadials, interstadials, and the Eemian, *J. Geophys. Res.*, this issue.
Ram, M., M. Illing, P. Weber, G. Koening, and M. Kaplan, Polar ice stratigraphy from laser light scattering: Scattering from ice, *Geophys. Res. Lett.*, *22*, 3525–3527, 1995.
Schøtt, C., E. D. Waddington, and C. F. Raymond, Predicted timescales for GISP2 and GRIP boreholes at Summit, Greenland, *J. Glaciol.*, *38*, 162–168, 1992.
Shuman, C. A., R. B. Alley, S. Anandakrishnan, and C. R. Stearns, An empirical technique for estimating near-surface air temperature trends in central Greenland from SSM/I brightness temperatures, *Remote Sens. Environ.*, *51*, 245–252, 1995.
Sowers, T., M. Bender, L. Labeyrie, D. Martinson, J. Jouzel, D. Raynaud, J. J. Pichon, and Y. S. Korotkevich, A 135,000-year Vostok-SPECMAP common temporal framework, *Paleoceanography*, *8*(6), 737–766, 1993.
Stuiver, M., P. M. Grootes, and T. Braziunas, The GISP2 $\delta^{18}O$ climate record of the past 16,500 years and the role of the sun, ocean, and volcanoes, *Quat. Res.*, *44*, 341–354, 1995.
Taylor, K., R. Alley, J. Fiacco, P. Grootes, G. Lamorey, P. Mayewski, and M. J. Spencer, Ice-core dating and chemistry by direct-current electrical conductivity, *J. Glaciol.*, *38*, 325–332, 1992.
Taylor, K. C., G. W. Lamorey, G. A. Doyle, R. B. Alley, P. M. Grootes, P. A. Mayewski, J. W. C. White, and L. K. Barlow, "The flickering switch" of late Pleistocene climate change, *Nature*, *361*, 432–436, 1993a.
Taylor, K. C., C. U. Hammer, R. B. Alley, H. B. Clausen, D. Dahl-Jensen, A. J. Gow, N. S. Gundestrup, J. Kipfstuhl, J. C. Moore, and E. D. Waddington, Electrical conductivity measurements from the GISP2 and GRIP Greenland ice cores, *Nature*, *366*, 549–552, 1993b.
Zielinski, G. A., Stratospheric loading and optical depth estimates of explosive volcanism over the last 2100 years derived from the GISP2 Greenland ice core, *J. Geophys. Res.*, *100*, 20,937–20,955, 1995.
Zielinski, G. A., P. A. Mayewski, L. D. Meeker, S. Whitlow, M. S. Twickler, M. Morrison, D. Meese, R. B. Alley, and A. J. Gow, Record of volcanism since 7000 B.C. from the GISP2 Greenland ice core and implications for the volcano-climate system, *Science*, *264*, 948–952, 1994.
Zielinski, G. A., M. S. Germani, G. Larsen, M. G. L. Baillie, S. Whitlow, M. S. Twickler, and K. Taylor, Evidence of the Eldgja (Iceland) eruption in the GISP2 Greenland ice core: Relationship to eruption processes and climatic conditions in the tenth century, *Holocene*, *5*, 129–140, 1995.
Zielinski, G. A., P. A. Mayewski, L. D. Meeker, K. Grönvold, M. S. Germani, S. Whitlow, M. S. Twickler, and K. Taylor, Volcanic aerosol records and tephrochronology of the Summit, Greenland, ice cores, *J. Geophys. Res.*, this issue.

R. B. Alley, Earth System Science Center, Pennsylvania State University, University Park, PA 16802.
J. F. Bolzan, Byrd Polar Research Center, Ohio State University, Columbus, OH 43210.
A. J. Gow and D. A. Meese, U.S. Army Cold Regions Research and Engineering Laboratory, Hanover, NH 03755. (e-mail: dmeese@hanover-crrel.army.mil)
P. M. Grootes, Leibniz-Labor, Christian-Albrechts-Universität Kiel, Max-Eyth-Strasse 11, 24118 Kiel, Germany.
P. A. Mayewski and G. A. Zielinski, Climate Change Research Center, Institute for the Study of Earth, Oceans and Space, University of New Hampshire, Durham, NH 03824.
M. Ram, Department of Physics, State University of New York at Buffalo, Buffalo, NY 14260.
K. C. Taylor, Desert Research Institute, University and Community College System of Nevada, Reno, NV 89506.

(Received February 3, 1996; revised December 22, 1996; accepted January 16, 1997.)